European Journal of Pharmaceutics and Biopharmaceutics 78 (2011) 117–124

Contents lists available at ScienceDirect

European Journal of Pharmaceutics and Biopharmaceutics

journal homepage: www.elsevier.com/locate/ejpb

Research paper

# A multivariate approach for the statistical evaluation of near-infrared chemical images using Symmetry Parameter Image Analysis (*SPIA*)

T. Puchert [a], D. Lochmann [b], J.C. Menezes [c], G. Reich [a,*]

[a] Institute of Pharmacy and Molecular Biotechnology, Department of Pharmaceutical Technology and Biopharmaceutics, University of Heidelberg, Germany
[b] Quality Operations, PAT – Laboratory, Merck Serono, Darmstadt, Germany
[c] Institute of Biotechnology and Bioengineering, Technical University of Lisbon, Portugal

ARTICLE INFO

*Article history:*
Received 5 July 2010
Accepted in revised form 22 December 2010
Available online 8 January 2011

*Keywords:*
NIR-CI
QbD
MVA
Homogeneity
Skewness
Kurtosis

ABSTRACT

Near-Infrared Chemical Imaging (NIR-CI) is rapidly gaining importance for the analysis of complex intermediate and final drug products. The availability of both spectral information from the sample and spatial information on the distribution of individual components offers access to greater understanding of manufacturing processes in many stages of pharmaceutical production. One major aspect in terms of chemical imaging is data analysis, since each measurement (image) generates a data cube containing several thousands of spectra (i.e., one spectrum per image pixel). The visual interpretation of component distribution (e.g., homogeneity) is an important issue but subjective. Chemometric methods are therefore required to extract qualitative and quantitative information from each image and enable comparison of several images. In this work, we describe a novel approach for the statistical evaluation of NIR-CI in terms of a multivariate treatment of univariate statistical descriptors characterizing image pixel (e.g., skewness and kurtosis). This technique was called by the authors "Symmetry Parameter Image Analysis" (*SPIA*), since it enables assessing the symmetry of pixel distributions in terms of different sample attributes. That approach is an innovative way of reporting results with a straightforward relation with attributes such as homogeneity, thus providing the basis for setting up acceptance criteria for good processing conditions or sample homogeneity. Furthermore, this procedure is applicable to determine product variability for large data sets without the need for explicit consideration of each image as its main attributes have been captured by the pixel distributions and their univariate descriptors.

The approach is described by means of data obtained by NIR-CI on a powder blend case study (*process application*). Additionally, *SPIA* was used for the qualitative classification of tablets (*sample application*), showing that the approach can be generalized to set up criteria for sample-to-sample similarity and be useful in establishing criteria for e.g., counterfeiting.



## 1. Introduction

Near-Infrared Chemical Imaging (NIR-CI) is becoming increasingly popular in the pharmaceutical industry. It is an emerging technique that combines conventional imaging and spectroscopy to attain both spatial information on the distribution of components and spectral information from an object. Reviews by Reich [1], Geladi et al. [2], Gendrin et al. [3], Gowen et al. [4] and book chapters by Griffiths [5], Lewis et al. [6] and Del Bianco et al. [7] comprehensively describe the basic principles, instrumentation, and analysis of NIR-CI. The relatively fast, non-destructive, and non-invasive features of NIR-CI mark its potential suitability as a Process Analytical Technology (PAT) tool for the pharmaceutical industry, for process monitoring, quality control, process development, root cause analysis, and trouble shooting in many stages of drug product manufacture [3,8–14]. The use of NIR-CI for the identification and characterization of counterfeit drug products has been described by Puchert et al. [15], Dubois et al. [16], and Wolff et al. [17]. Core to the PAT initiative is the Quality by Design (QbD) concept; rather than being tested into products and manufacturing processes, quality should be built in [18–20]. In this context, it is mentioned that blend homogeneity is essential to obtain high quality products of uniform drug content. Studies for the monitoring of powder blend homogeneity using NIR-CI were published by El-Hagrasy et al. [18] and Lewis et al. [19], while studies by Lyon et al. [20] and Westenberger et al. [21] dealt with tablet homogeneity. What they have in common is the usage of the standard deviation of pixel intensity distribution of single channel images for the image analysis to determine homogeneity. Additionally,

* Corresponding author. Institute of Pharmacy and Molecular Biotechnology, Department of Pharmaceutical Technology and Biopharmaceutics, University of Heidelberg, Germany. Tel.: +49 (0) 6221 54 8335; fax: +49 (0) 6221 54 5971.
*E-mail address:* gabriele.reich@urz.uni-heidelberg.de (G. Reich).

0939-6411/$ - see front matter © 2011 Elsevier B.V. All rights reserved.
doi:10.1016/j.ejpb.2010.12.035

Lyon et al. [20] and Ravn et al. [22] have used PLS predicted images instead of single channel images for the determination of tablet homogeneity. Furthermore, symmetry parameters like *Skewness* and *Kurtosis* (both are measures of normality in terms of statistical normal distribution) given by image histogram statistics were used by Lewis et al. [19] in an univariate manner for data analysis and interpretation of homogeneity.

Major aspects in terms of chemical imaging are data analysis and data mining. Most images have a strong visual content, and visual interpretation is very important [2]. It is, however, subjective, since for process monitoring or batch comparison, hundreds or even thousands of images have to be analysed. Statistical tools are therefore required for data reduction and reporting. Image analysis using parameters such as standard deviation, skewness, or kurtosis in an univariate manner is difficult to interpret, most notably if some samples differ in terms of content and are evenly distributed with low standard deviation, while other samples have large skewness values but non-significant changes in kurtosis or vice versa. Due to the different nature of sample variability, a general assessment is not feasible. To overcome this problem, we developed a novel multivariate approach of Symmetry Parameter Image Analysis (*SPIA*). Additionally, an innovative method for the statistical reporting was applied. The techniques are described using a powder blend case study (*process application*) and a qualitative classification study of tablets (*sample application*).

## 2. Materials and methods

### 2.1. Powder blend case study (process application)

A 100 L bin-blender (Servolift GmbH, Offenburg, Germany) was charged with one low dose active pharmaceutical ingredient (API) (~2.5% w/w drug loading and a mean particle size of 40 μm) and four excipients (Crospovidone, Microcrystalline Cellulose, Corn Starch and Magnesium Stearate). All ingredients were of the highest available pharmaceutical grade and complied with their corresponding European Pharmacopoeia monographs. The blender fill level was set to 85% of the total vessel volume, and the components were mixed for 1 h at 12 rpm. The blending process was stopped at pre-defined time intervals (1, 3, 5, 7, 9, 11, 13, 15, 17, 19, 21, 23, 25, 27, 29, 60 min). Aliquots comparable to one tablet mass were withdrawn at five different powder bed locations within the vessel using a sample thief to be analysed by NIR-CI.

In this context, it should be mentioned that the current state of the art approach of collecting blend samples by using sampling thieves can result in significant sampling errors or bias, since the orientation, angle, and depth of sampling thief insertion, as well as insertion force and smoothness, impact the consistency of the sampling. Such sampling devices disturb the powder bed and compromise the validity of collected samples [18,23]. Sampling has been carried out carefully, and the sampling protocol was consistent throughout the study.

### 2.2. Near-Infrared Chemical Imaging (NIR-CI)

Data were collected with a SyNIRgi™ Chemical Imaging System (Malvern Instruments, Malvern, UK) equipped with an InSb focal plane array detector (320 × 256 pixels) and a 30-position automatic sample holder. Image cubes of each powder sample were acquired with Pixys® 1.1 software (Malvern Instruments, Malvern, UK) in the spectral range 1200–2400 nm at 10 nm steps and 16 frames per wavelength. The field of view was set to 12.8 × 10.2 mm which encompasses 100% of the area of the sample and provides a magnification of 40 μm per pixel. Each image cube contained 81 920 full NIR spectra and required a collection time of approximately 3 min. Before the actual sample is scanned, the software enforces the collection of appropriate dark and background data cubes and then uses these data to produce reflectance spectra according to the formula $R = (S - D)/(B - D)$, where $S$ is the sample cube, $B$ is the 99% reflectance cube (Background), $D$ is the dark cube, and $R$ is the resulting reflectance cube. This calculation was performed for all pixels in all planes in the cube.

The first step was to convert the data into absorbance units according to the following equation: $A = \log 1/R$, where $A$ = absorbance and $R$ = reflectance. Non-sample regions were masked, and a standard normal variate (SNV) algorithm [24] followed by a first derivative was applied (Savitzky–Golay algorithm [25], using second-order polynomials across 21 data points). Furthermore, pure component spectra were collected from powder samples of the API and pharmaceutical-grade Crospovidone, Microcrystalline Cellulose, Corn Starch and Magnesium Stearate to build a hyperspectral reference library. Spectral data of all five components were processed in the same manner.

A reference library with >600 spectra per component was built for the API and the excipients. These training spectra were used as predictors to build a partial least squares (PLS) classification model, which was applied to the spectral data of the powder blend samples for discriminant analysis. Applying such PLS model to the powder blend samples resulted in a "classification scores image" for each of the library components without any quantitative calibration set being required. The intensity of each pixel in the resultant predicted classification scores image is determined by the degree of membership (scaled from 0 to 1) predicted for the spectrum at that special location based on the reference. A score value of 0 meant that the component was not present, and a score value of 1 meant that the component was present at 100%. The brighter the colour of the pixel, the stronger the degree of membership of that spectrum to the specific class, predicted at that location. For the presented images, the brighter colour represents a higher concentration. The variation in predicted classification scores and the distribution of pixels reflects the variation in component concentration across the sample and is an indication for homo- or heterogeneity of spectra [13]. All PLS predicted images shown in the next section result from histogram plots centred to the mean and normally distributed. The predicted concentration threshold was set to 3SD.

### 2.3. Qualitative classification study of tablets (sample application)

Tablets from five different manufacturers (no counterfeits) with the same content of an API (~2.5% w/w drug loading) but differences in the excipient composition were used. Five samples from

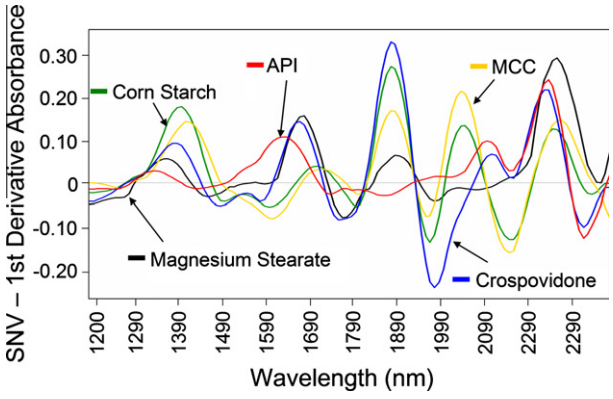


**Fig. 1.** Pre-treated mean spectra of pure components. (For interpretation of the references to colour in this figure legend, the reader is referred to the web version of this article.)

each batch were analysed. Coating was carefully removed using a scalpel in order to expose the interior to NIR-CI.

### 2.4. Data analysis

Imaging data were analysed and processed with ISys 5.0 software (Malvern Instruments, Malvern, UK). The results from histogram statistics were processed and visualized using the software SIMCA-P+ 12.0 (Umetrics, Umeå, Sweden).

## 3. Results and discussion

### 3.1. Powder blend NIR-CI analysis

The first step was the development of the reference library and the PLS calibration model with the powder samples of the pure API and four major NIR-active excipients (Crospovidone, Microcrystalline Cellulose, Corn Starch and Magnesium Stearate). Pre-treated mean spectra of the pure raw materials are shown in Fig. 1.

As the purpose of the study was to establish a fast method for discriminant analysis, a PLS classification model rather than a quantitative PLS model was developed. A model with five factors was sufficient for the reliable discrimination of ingredients (one API and four other excipient components). The Predicted Residual Sum of Squares (PRESS) was lower than 0.02 at that stage (PRESS displays how the residual prediction errors depend on the number of factors in the model). We truncated the factors beyond five, because the slope of the PRESS significantly flattens.

The next step was to apply the PLS model to all powder blend samples (see Section 2.1: samples were withdrawn at different powder bed locations within the vessel). Fig. 2 shows the PLS predicted API images – "five samples at a time". The score values over the images show that the maximum value at any pixel is only ~0.025 which would equate to an abundance of ~2.5%, i.e., 97.5% of the pixel contribution is from the other components.

The distribution of the API showed strong variability within the samples. Samples from the beginning (A1–E1) differed with respect to the relative abundance of the API, while samples from the end of the blend process clearly varied in the spatial distribution. Generally, samples within the time period of 3 min (A3–E3) up to 17 min (A17–E17) were evenly distributed, which indicated good homogeneity. In this case, it was obvious that unnecessarily long mixing significantly affected quality. Shah and Mlodozeniec [26], in their study of surface lubrication phenomena, suggested that during the mixing process, lubricant particles such as

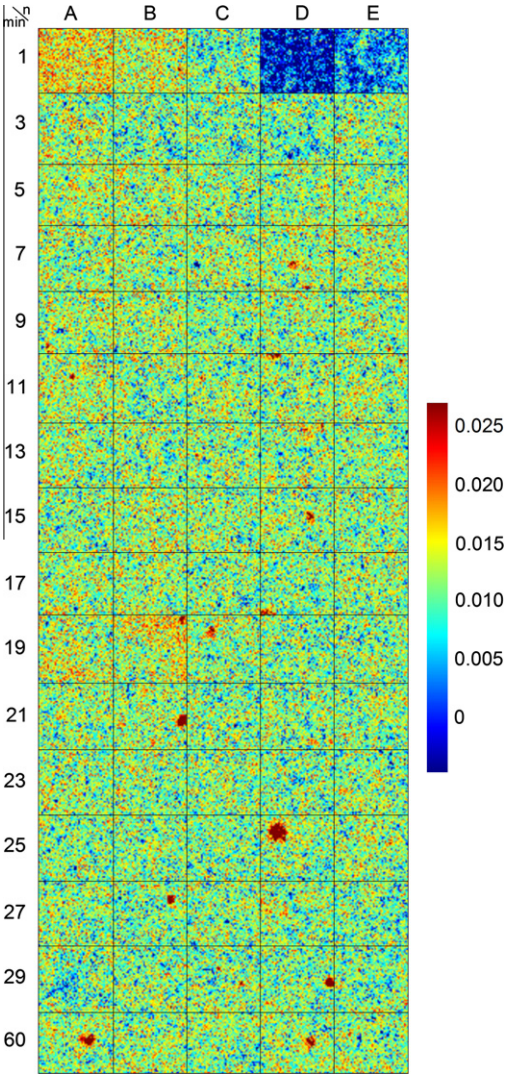


**Fig. 2.** PLS predicted API images. (For interpretation of the references to colour in this figure legend, the reader is referred to the web version of this article.)

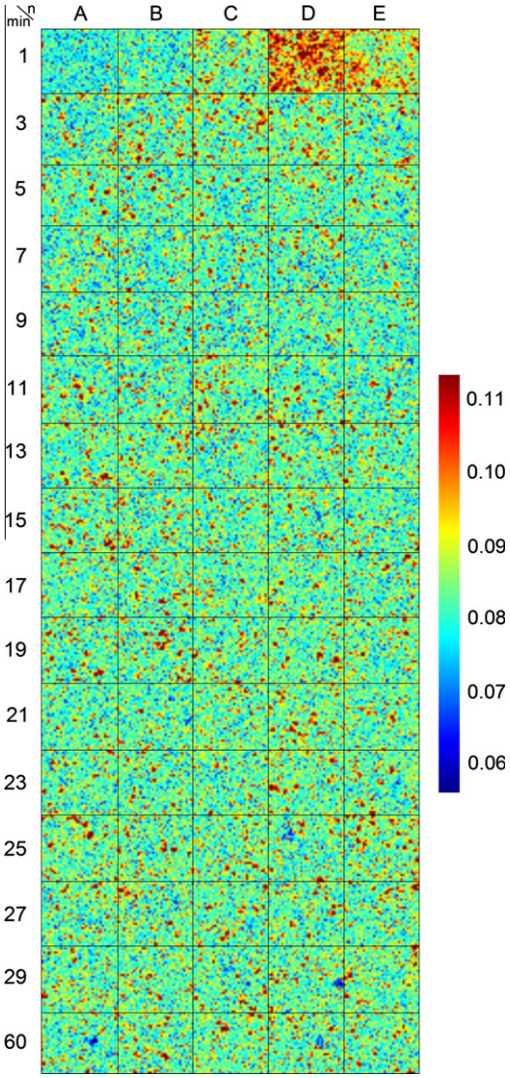


**Fig. 3.** PLS predicted Crospovidone images. (For interpretation of the references to colour in this figure legend, the reader is referred to the web version of this article.)

Magnesium Stearate first adsorb onto the surface of individual powder particles or granules and then, as mixing continues, distribute more uniformly upon the granule surface following delamination or deagglomeration mechanisms [27]. Segregation or lubrication phenomena are not discussed in more detail at this point, since the statistical analysis of chemical images was the focus of the study.

Figs. 3–6 illustrate the PLS predicted images of the major excipients. The visual inspection of the images also indicated differences in the relative abundance and spatial distribution of components.

Lyon et al. [20] described homogeneity measurements by calculating the % standard deviation of the distribution of the predicted classification scores for a given component within a specimen. Homogeneous samples will have small standard deviations, while heterogeneous samples will have larger standard deviations. In this study, the % standard deviation was calculated as follows (1):

$$\%std = v = \frac{s}{\bar{x}} \cdot 100 \tag{1}$$

where $s$ is the standard deviation and ($\bar{x}$) the mean value of pixel intensity distribution throughout the image.

Image statistics was carried out, but the % standard deviation of the predicted classification scores was less sensitive. Fig. 7 illustrates the % standard deviation of the API. The values decreased after 3 min to a certain minimum. There were no major differences observable until the end of the blend process contrary to the visual inspection of the PLS predicted API images.

A new statistical approach was used to analyse sample variability with the aim to gain higher sensitivity for image analysis, thus providing the basis for setting up acceptance criteria for good processing conditions or sample homogeneity. The approach will be described in more detail in the next section.

### 3.1.1. Novel approach of Symmetry Parameter Image Analysis (SPIA)

The approach is shown schematically in Fig. 8.

First, we performed a descriptive statistical analysis at the sample (image) level. This resulted in PLS predicted images, as previously described. Through histogram plots and statistics patterns, the predicted classification scores and pixel distribution throughout the image were computed. Parameters given by the histogram plot are the mean, standard deviation, skewness, and kurtosis of pixel intensity distribution throughout the image of a component. They are related to intra-sample homogeneity and can be used to compare different samples or assess sample-to-sample variability from same or a different process as in blending or counterfeit testing, respectively.

Skewness is a measure of the lack of symmetry. A distribution, or data set, is symmetric if its mean and median match (i.e., if it

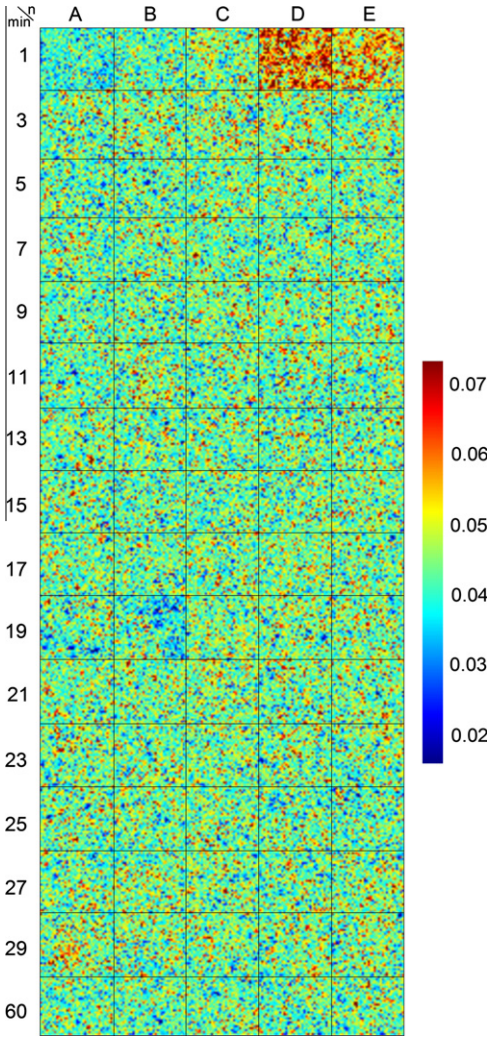


**Fig. 4.** PLS predicted Microcrystalline Cellulose images. (For interpretation of the references to colour in this figure legend, the reader is referred to the web version of this article.)

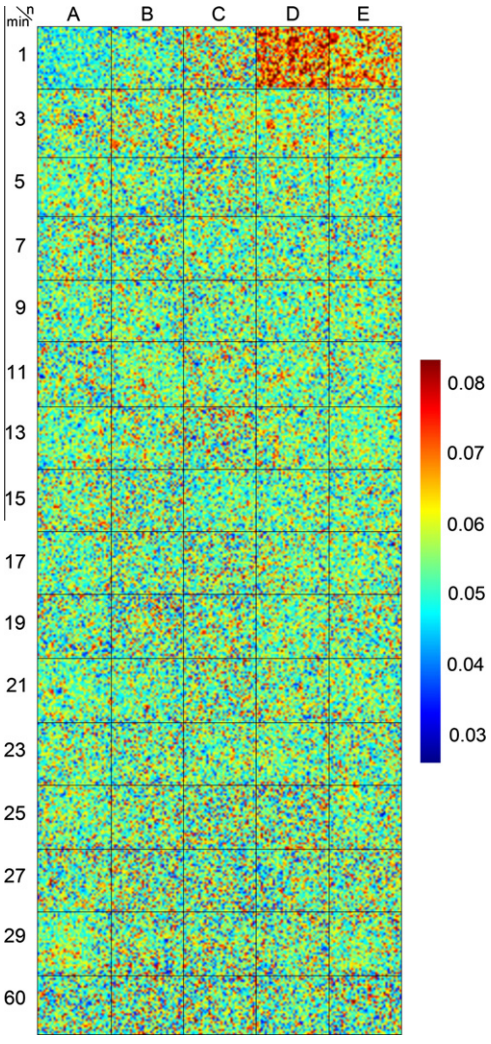


**Fig. 5.** PLS predicted Corn Starch images. (For interpretation of the references to colour in this figure legend, the reader is referred to the web version of this article.)

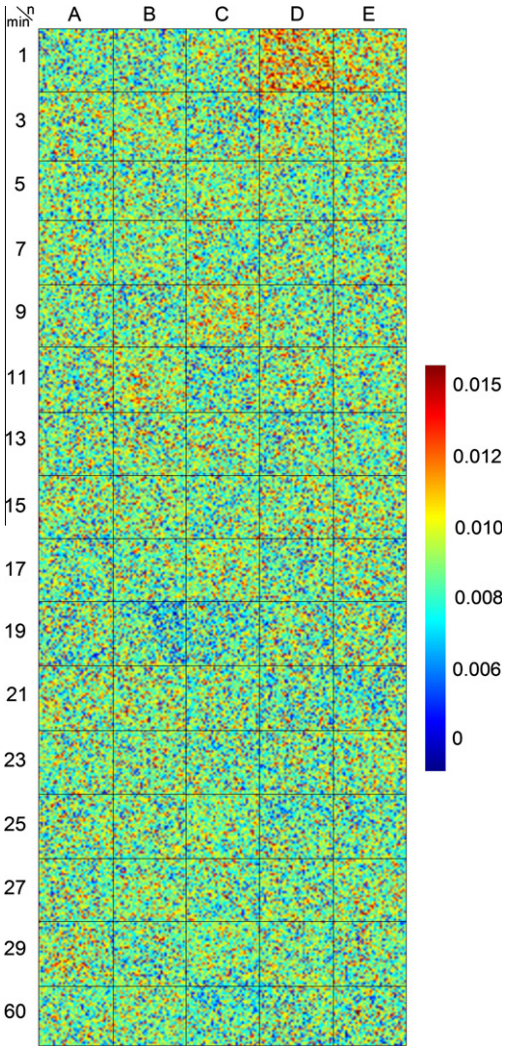


**Fig. 6.** PLS predicted Magnesium Stearate images. (For interpretation of the references to colour in this figure legend, the reader is referred to the web version of this article.)

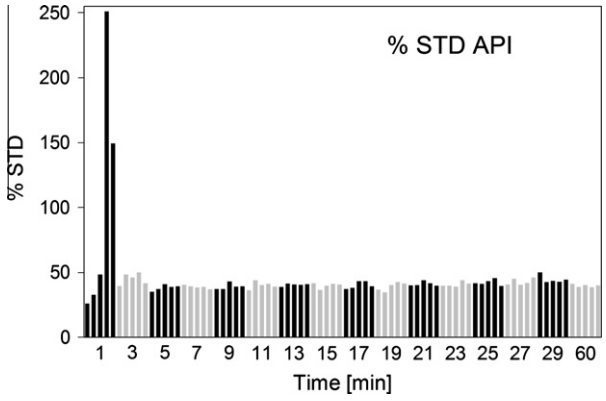


**Fig. 7.** % Standard deviation of the API.

looks the same to the left or to the right of the location of the mean). The skewness for a normal distribution is zero, and any reasonably symmetric data set should have a skewness near zero. Negative values for the skewness indicate data that are left skewed, while positive values indicate that the distribution is right

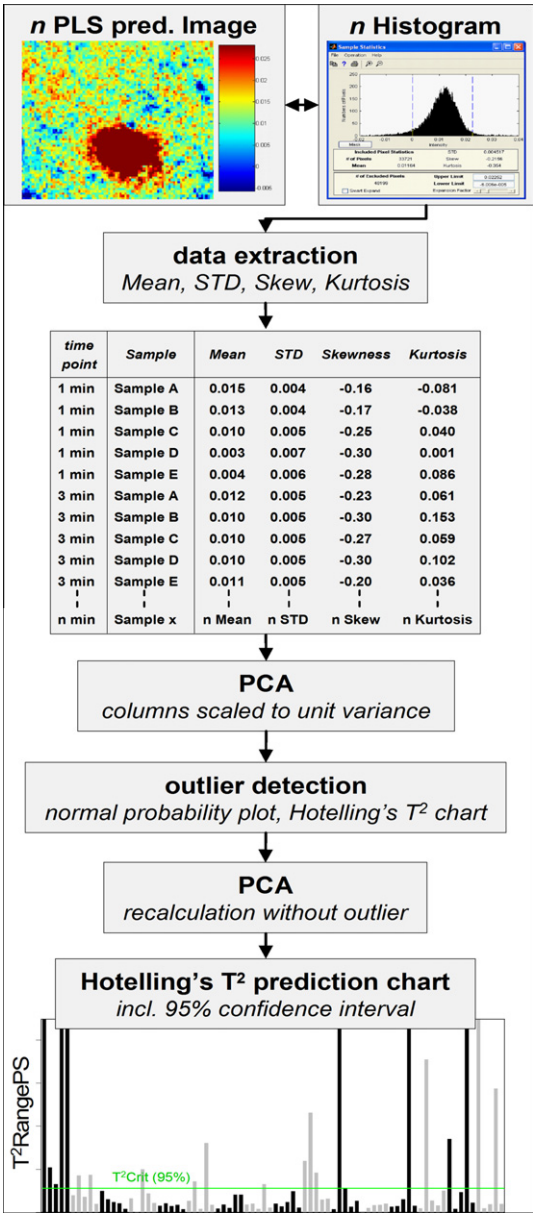


**Fig. 8.** Description of Symmetry Parameter Image Analysis (*SPIA*). (For interpretation of the references to colour in this figure legend, the reader is referred to the web version of this article.)

skewed. By skewed to the left, we mean that the left tail is long relative to the right tail.

Kurtosis is a measure of whether the data are peaked or flat relative to a normal distribution. Positive kurtosis indicates a "peaked" distribution, and negative kurtosis indicates a flattened distribution [28].

As described in Section 2, the threshold of each histogram was set to 3SD from the mean. The mean value and the corresponding standard deviation, skewness, and kurtosis values of each PLS predicted image were exported to a spreadsheet. This resulted in columns of the mean (=relative abundance), standard deviation, skewness, and kurtosis values of each component (API and four excipients) for the defined time intervals (rows). It should be mentioned that we also performed multivariate data analysis with the histograms – comparable to analysing spectral data. However, the results were not meaningful to describe significant variability (data not shown).

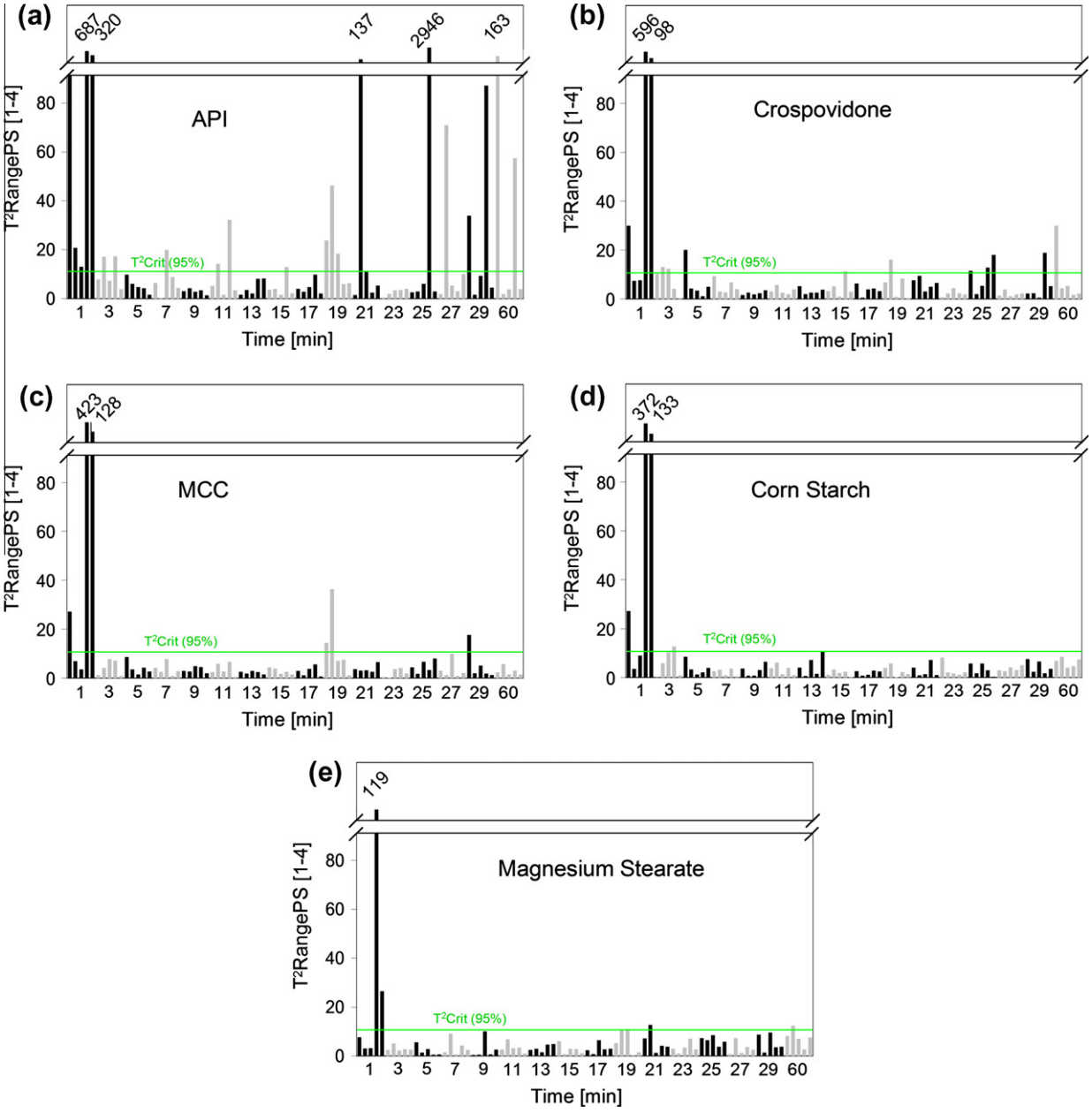


**Fig. 9.** Predicted Hotelling's $T^2$ chart for: (a) API; (b) Crospovidone; (c) Microcrystalline Cellulose; (d) Corn Starch; (e) Magnesium Stearate. (For interpretation of the references to colour in this figure legend, the reader is referred to the web version of this article.)

The current approach to illustrate variability is to plot the parameters given by the histogram statistics separately into univariate control charts. Some samples, for example, differ in terms of content and are evenly distributed with low standard deviation. Other samples have large skewness values but non-significant changes in kurtosis or vice versa. Due to the different nature of sample variability, a general assessment is not feasible. To overcome this problem, we performed principal component analysis (PCA) on all parameters given by the histogram plot of the PLS predicted images. PCA is probably the most widespread multivariate statistical technique used in chemometrics [29]. An important issue, regarding PCA, is the choice of the scale. It is well known that it is compulsory to use scale when the variables are of different nature (e.g., temperature and pressure) [30]. This is relevant here, since kurtosis and skewness are different in nature. Each column of the tables was centred and scaled to unit variance (autoscaling), by subtracting each value in the column by the mean and dividing each value in the column by the standard deviation. If data are scaled to unit variance, the weighting reflects their correlation, while using mean centring the weighting reflects the covariance of the variables [31]. Five independent PCA models were built - one for each chemical component in a sample. This approach is meaningful, since different blend dynamics of ingredients were observable.

The calculations of each PCA model revealed that four principal components (PC) were sufficient to explain about 99% of the variability in the data. A multivariate method that is the multivariate counterpart of Student's *t*-test and which also forms the basis for certain multivariate control charts is based on Hotelling's $T^2$ distribution, which was introduced by Hotelling [32]. The $T^2$ control chart is a tool to detect multivariate outliers, mean shifts, and other distributional deviations from the in-control distribution. It has to be mentioned that Hotelling's $T^2$ statistics is commonly available in 21 CFR Part11 certified standard chemometric software and there-

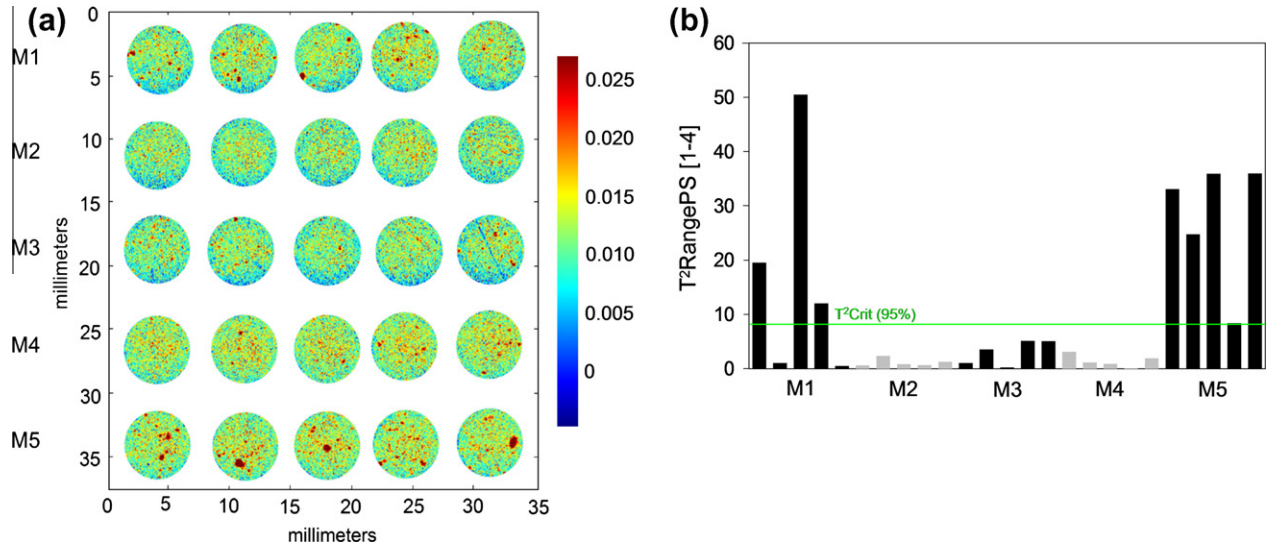


**Fig. 10.** (a) PLS predicted API images of tablets from five manufacturers; (b) predicted Hotelling's $T^2$ chart for tablets from different manufacturers. (For interpretation of the references to colour in this figure legend, the reader is referred to the web version of this article.)

fore used in this study. By plotting the PCA results including the four PCs for each ingredient (API and excipients) into Hotelling's $T^2$ control charts, some outliers were detected. Usually it is assumed that a series of measurements fall roughly into a normal distribution. If some measurements are so extreme that they cannot easily be accounted for this way, they are probably outliers [33]. In our case, samples D1 and E1 were most likely outliers in all data sets – that was already observable by visual inspection of the images. If they were retained in the datasets, they would disturb an otherwise close to normal distribution. Therefore, we excluded the outliers in each data set and recalculated all PCA models. In our case, Hotelling's $T^2$ 95% confidence intervals were chosen. For each PLS predicted image, it can be determined, whether it falls within or outside the confidence limit. Fig. 9 illustrates the predicted Hotelling's $T^2$ charts for each ingredient.

The Hotelling's $T^2$ chart results confirmed the findings of image visualization. Samples outside the 95% confidence interval in the $T^2$ charts also showed significant image characteristics related to inhomogeneity. The PLS predicted images of the API showed the largest variance in terms of pixel intensity and spatial distribution, while the excipients were more or less evenly distributed. Consequently, we defined the API as limiting factor to describe blend homogeneity. In this example, the blend reached homogeneity within 3 min, while segregation or lubrication phenomena occurred after 17 min.

### 3.2. Tablet NIR-CI analysis

The motivation of the study was to demonstrate the potential of Symmetry Parameter Image Analysis (*SPIA*) also being applicable to compare solid drug products (e.g., tablets from different manufacturers) in terms of API distribution. Image acquisition and pretreatments were processed in the same manner as for the powder blend study. The previously developed hyperspectral reference library and PLS calibration model were applied to the tablet samples with the difference that only the PLS predicted API images were used for further investigation.

We followed the new approach as described in the previous section, but this time, we used manufacturer-related samples instead of time-related samples to be analysed by PCA and Hotelling's $T^2$ statistics. The results are shown in Fig. 10.

The PLS predicted API images of manufacturer M1 and M5 showed the largest variance in terms of pixel intensity and spatial distribution, while tablets of manufacturer M2, M3, and M4 were evenly distributed (Fig. 10a). This was confirmed by the $T^2$ chart (Fig. 10b).

The complementarity between "process application" and "sample application" clearly demonstrates the potential of *SPIA* in being general and applicable in the future to set up criteria for various types of applications.

## 4. Conclusions

A new multivariate approach for the statistical evaluation of NIR-CI was developed. This type of image analysis is called by the authors Symmetry Parameter Image Analysis (*SPIA*). Based on a powder blend study, it was shown that the current practice of calculating the % standard deviation for a given component within a specimen was not sensitive enough to assess blend uniformity. By using symmetry parameters such as skewness and kurtosis together with mean and standard deviation in a multivariate manner, reliable determination of blend homogeneity was achieved. The approach of reporting results given by Principal Component Analysis in a Hotelling's $T^2$ chart confirmed the findings of image visualization. This also provides an elegant way for data reduction since image visualization is time consuming and in the case of hundreds or even thousands of images not feasible. We have also shown that different blend dynamics of ingredients can be evaluated under these criteria, since NIR-CI delineates the spatial uniformity of the API as well as major excipients across the sample.

Additionally, *SPIA* has demonstrated to be suitable and straightforward for the assessment of solid drug products in the context of a sample application. Based on tablets from five different manufacturers, a classification in terms of the API distribution has been carried out. We observed extreme differences between the various manufacturers by applying the novel approach of data analysis. Of course, such a small sample set is not conclusive, but the magnitude of differences found suggests that this should be investigated further. In this context, the use of *SPIA* for the detection of counterfeit drug products is conceivable by setting criteria for counterfeiting, i.e., dissimilarity between a suspect sample and a reference genuine sample.

At-line NIR-CI together with *SPIA* fully complies with the PAT concept and the QbD principles in terms of gaining process understanding. In the future, hundreds or even thousands of images could be analysed by applying *SPIA* to on-line NIR-CI systems. In

this context, further investigations need to be carried out to exploit the full potential and assess the limitations of this approach for use in on-line process monitoring. In general, using parameters given by image histogram statistics in combination with multivariate data analysis is a powerful PAT tool to detect sample or product variability. It can help to evaluate process capability in the many stages of drug product manufacture with a potential impact on better process control and towards improved quality by process design and operation in line with the *International Conference on Harmonization* (ICH) Q8 [34] guideline.

## Acknowledgments

The authors want to thank Dr. Jens Schewitz for his careful review of the manuscript and helpful discussion and Dr. Daniel von Bamberg (both from Merck Serono) for his overall support of the project.

## References

[1] G. Reich, Near-infrared spectroscopy and imaging: basic principles and pharmaceutical applications, Adv. Drug Deliv. Rev. 57 (2005) 1109–1143.
[2] P. Geladi, B. Sethson, J. Nyström, T. Lillhonga, T. Lestander, J. Burger, Chemometrics in spectroscopy. Part 2. Examples, Spectrochim. Acta, Part B 59 (2003) 1347–1357.
[3] C. Gendrin, Y. Roggo, C. Collet, Pharmaceutical applications of vibrational chemical imaging and chemometrics: a review, J. Pharm. Biomed. Anal. 48 (2008) 533–553.
[4] A.A. Gowen, C.P. O'Donnell, P.J. Cullen, S.E.J. Bell, Recent applications of chemical imaging to pharmaceutical process monitoring and quality control, Eur. J. Pharm. Biopharm. 69 (2008) 10–23.
[5] P.R. Griffiths, Infrared and Raman instrumentation for mapping and imaging, in: R. Salzer, H.W. Siesler (Eds.), Infrared and Raman Spectroscopic Imaging, Wiley-VCH, Weinheim, DE, 2009, pp. 3–64.
[6] E.N. Lewis, J.W. Schoppelrei, E. Lee, L. Kidder, Near-infrared chemical imaging as a process analytical tool, in: K. Bakeev (Ed.), Process Analytical Technology, Blackwell Publishing Ltd., Oxford, UK, 2005, pp. 187–225.
[7] A. Del Bianco, A. Kurzmann, R. Kessler, Bildgebende optische und spektroskopische Verfahren, in: R. Kessler (Ed.), Prozessanalytik, Wiley-VCH, Weinheim, DE, 2006, pp. 313–339.
[8] F. Clarke, Extracting process-related information from pharmaceutical dosage forms using near infrared microscopy, Vib. Spectrosc. 34 (2004) 25–35.
[9] E.N. Lewis, J. Schoppelrei, E. Lee, Near-infrared chemical imaging and the PAT initiative, Spectroscopy 4 (2004) 26–34.
[10] E. Lee, H.W. X, P. Chen, E.N. Lewis, R.V. Vivilecchia, High-throughput analysis of pharmaceutical tablet content uniformity by near-infrared chemical imaging, Spectroscopy 21 (2006) 24–31.
[11] Y. Roggo, A. Edmond, P. Chalus, M. Ulmschneider, Infrared hyperspectral imaging for qualitative analysis of pharmaceutical solid forms, Anal. Chim. Acta 535 (2005) 79–87.
[12] J. Dubois, E.N. Lewis, Advanced Troubleshooting of Dissolution Failure, 2009, pp. 38–45, <www.pharmaceuticalonline.com>.
[13] L. Makein, L.H. Kidder, E.N. Lewis, M. Valleri, Non-destructive evaluation of manufacturing process changes using near infrared chemical imaging, NIR News 19 (2008) 11–15.
[14] Y. Roggo, N. Jent, A. Edmond, P. Chalus, M. Ulmschneider, Characterizing process effects on pharmaceutical solid forms using near-infrared spectroscopy and infrared imaging, Eur. J. Pharm. Biopharm. 61 (2005) 100–110.
[15] T. Puchert, D. Lochmann, J.C. Menezes, G. Reich, Near-infrared chemical imaging (NIR-CI) for counterfeit drug identification – a four-stage concept with a novel approach of data processing (Linear Image Signature), J. Pharm. Biomed. Anal. 51 (2010) 138–145.
[16] J. Dubois, J.-C. Wolff, J.K. Warrack, J. Schoppelrei, E.N. Lewis, NIR chemical imaging for counterfeit pharmaceutical products analysis, Spectroscopy 2 (2007) 40–46.
[17] J.-C. Wolff, J.K. Warrack, L. Kidder, E.N. Lewis, NIR-based chemical imaging as an anticounterfeiting tool, Pharm. Manuf. 7 (2008) 27–31.
[18] A.S. El-Hagrasy, H.R. Morris, F. D'Amico, R.A. Lodder, J.K. Drennen 3rd, Near-infrared spectroscopy and imaging for the monitoring of powder blend homogeneity, J. Pharm. Sci. 90 (2001) 1298–1307.
[19] E.N. Lewis, L.H. Kidder, E. Lee, NIR chemical imaging as a process analytical tool, Inn. Pharm. Tech. (2006) 1–5.
[20] R.C. Lyon, D.S. Lester, E.N. Lewis, E. Lee, L.X. Yu, E.H. Jefferson, A.S. Hussain, Near-infrared spectral imaging for quality assurance of pharmaceutical products: analysis of tablets to assess powder blend homogeneity, AAPS PharmSciTech 3 (2002) 1–15.
[21] B.J. Westenberger, C.D. Ellison, A.S. Fussner, S. Jenney, R.E. Kolinski, T.G. Lipe, R.C. Lyon, T.W. Moore, L.K. Revelle, A.P. Smith, J.A. Spencer, K.D. Story, D.Y. Toler, A.M. Wokovich, L.F. Buhse, Quality assessment of internet pharmaceutical products using traditional and non-traditional analytical techniques, Int. J. Pharm. 306 (2005) 56–70.
[22] C. Ravn, E. Skibsted, R. Bro, Near-infrared chemical imaging (NIR-CI) on pharmaceutical solid dosage forms—comparing common calibration approaches, J. Pharm. Biomed. Anal. 48 (2008) 554–561.
[23] T. Allen, Powder sampling, in: T. Allen (Ed.), Powder Sampling and Particle Size Determination, Elsevier B.V., Amsterdam, NL, 2003, pp. 1–55.
[24] R.J. Barnes, M.S. Dhanoa, S.J. Lister, Standard normal variate transformation and de-trending of near-infrared diffuse reflectance spectra, Appl. Spectrosc. 43 (1989) 772–777.
[25] A. Savitzky, H.J.E. Golay, Smoothing and differentiation of data by simplified least squares procedures, Anal. Chem. 36 (1964) 1627–1639.
[26] A.C. Shah, A.R. Mlodozeniec, Mechanism of surface lubrication: influence of duration of lubricant-excipient mixing on processing characteristics of powders and properties of compressed tablets, J. Pharm. Sci. 66 (1977) 1377–1382.
[27] D.J. Wargo, J.K. Drennen, Near-infrared spectroscopic characterization of pharmaceutical powder blends, J. Pharm. Biomed. Anal. 14 (1996) 1415–1423.
[28] NIST/SEMATECH, e-Handbook of Statistical Methods, 2010. <http://www.itl.nist.gov/div898/handbook/>.
[29] R.G. Brereton, Principal components analysis: the method, in: R.G. Brereton (Ed.), Chemometrics – Data Analysis for the Laboratory and Chemical Plant, John Wiley & Sons, Ltd., Chichester, UK, 2003, pp. 191–223.
[30] J. Collet, X. Epiard, P. Coudray, Simulating hydraulic inflows using PCA and ARMAX, Eur. Phys. J. Specl. Top. 174 (2009) 125–134.
[31] A. Craig, O. Cloarec, E. Holmes, J.K. Nicholson, J.C. Lindon, Scaling and normalization effects in NMR spectroscopic metabonomic data sets, Anal. Chem. 78 (2006) 2262–2267.
[32] H. Hotelling, Analysis of a complex of statistical variables into principal components, J. Educ. Psychol. 24 (1933). 417–441 and 498–520.
[33] R.G. Brereton, Detection of outliers, in: R.G. Brereton (Ed.), Applied Chemometrics for Scientists, John Wiley & Sons, Ltd., Chichester, UK, 2007, pp. 100–103.
[34] International Conference on Harmonisation, ICH Q8: Pharmaceutical Development: Step 4, 2006.